Original research

Preclinical feasibility study for transvascular drainage of non-acute subdural hematomas

Yang Liu ,[1,2] Sarosh Irfan Madhani ,[2,3] Jorge Luis Arturo Larco,[2,4] Adnan Hussain Shahid ,[2,5] Yigit Can Senol ,[3] Pedro N Lylyk,[2,6] Luis Savastano[2,3]

► Additional supplemental material is published online only. To view, please visit the journal online (https://doi.org/10.1136/jnis-2025-023794).

[1]Global Institute of Future Technology, Shanghai Jiao Tong University, Shanghai, China
[2]Department of Neurosurgery, Mayo Clinic, Rochester, Minnesota, USA
[3]Department of Neurological Surgery, University of California San Francisco, San Francisco, California, USA
[4]Radiology, UT Southwestern Medical Center, Dallas, Texas, USA
[5]Neurosurgery, University of South Alabama, Mobile, Alabama, USA
[6]Interventional Neuroradiology, Instituto Medico ENERI, Buenos Aires, Argentina

Correspondence to
Dr Luis Savastano; luis.savastano@ucsf.edu

Received 29 May 2025
Accepted 14 July 2025

ABSTRACT

Background Non-acute or chronic subdural hematoma (cSDH) is commonly treated with surgical evacuation followed by middle meningeal artery embolization (MMAe). This two step approach increases procedural complexity and redundancy, hospitalization duration, and patient risk. We hypothesized that cSDH could be managed through a single session endovascular procedure and conducted a multimodal preclinical study to evaluate feasibility.

Methods We performed three-dimensional heat mapping of hematoma distribution from preoperative CT scans (n=69) and analyzed middle meningeal artery (MMA) and superior sagittal sinus (SSS) anatomy and perforation trajectories using imaging from 107 patients. Rheological properties of 41 SDH samples were assessed using hybrid rheometry and modeled with the Carreau equation. Aspiration feasibility was tested using a 0.027 inch microcatheter (n=16), and dura perforation forces were quantified with a 28 G needle in fresh cadaveric dura (n=10).

Results Heat mapping localized cSDH to the parietal convexities (>80% probability) under the branches of the MMA, with limited midline involvement and proximity to the SSS (<10%). The posterior division of the MMA (diameter 1.23±0.23 mm) accommodated a 0.027 inch microcatheter in >90% of cases, with perforation trajectories targeting high probability hematoma zones in 105 of 107 cases. SDH samples exhibited shear thinning viscosity (η_0=172 mPa×s, η_∞=2.78 mPa×s), with mean aspiration times of 1.21±0.54 min per 10 mL. Perforation forces averaged 0.68±0.24 N in normal and 1.29±0.48 N in calcified dura (P=0.05).

Conclusion Anatomical, rheological, and biomechanical data from this study support the feasibility of endovascular drainage of cSDH through the MMA.

WHAT IS ALREADY KNOWN ON THIS TOPIC

⇒ Chronic subdural hematoma (cSDH) has high recurrence and mortality rates despite surgical evacuation.
⇒ Surgical drainage and adjuvant middle meningeal artery embolization (MMAe) are associated with a decrease in cSDH recurrence but an increase in costs, hospitalization, and risks.

WHAT THIS STUDY ADDS

⇒ Topographic analysis of operative non-acute SDH.
⇒ Rheological analysis of non-acute SDH with radiographic correlation.
⇒ Biomechanical analysis of the human dura.
⇒ Preclinical feasibility of endovascular cSDH drainage.

HOW THIS STUDY MIGHT AFFECT RESEARCH, PRACTICE, OR POLICY

⇒ This study provides the foundational data to develop a catheter based technology for transvascular cSDH drainage.

INTRODUCTION

Non-acute or chronic subdural hematoma (cSDH) is a collection of blood on the brain's surface that generally begins forming weeks after head trauma and expands, with the potential to cause brain compression, neurologic deficits, and death, increasing in frequency each year.[1] In the US, cSDH affects 17–20 per 100 000 individuals each year,[2] with increased incidence in patients aged >65 years and with the use of anticoagulation and/or antiplatelet agents.[3] To date, cSDH has an inhospital mortality rate of 16.7%, a 1 year mortality rate of 32% with only 21.1% of patients admitted returning home,[4 5] and is associated with a marked reduction in the patient's life expectancy compared with age matched controls.[6]

Surgical evacuation, including twist drill hole, burr hole, and craniotomy based evacuations, is the gold standard treatment for symptomatic cSDH.[7] Unfortunately, surgical evacuation of cSDH, although initially effective for most patients, fails to cure up to 37% of patients, with most recurrence rates in the range 10–20%.[8–13] Even when treatment fails once and patients undergo repeat surgical treatment, further recurrences are common, with a rate as high as 46%.[14] Surgical drainage is commonly combined with the introduction of drains in the subdural space, which remain in place for 2–3 days. This strategy is successful in reducing the recurrence rate by half but requires prolonged stays in the intensive care unit and is associated with a brain infection rate >7%.[15] In addition, open surgical interventions necessitate the complete reversal of antiplatelet and anticoagulant agents for weeks, which are concomitant medications in a large proportion of cSDH patients, thus potentially subjecting these patients to serious ischemic complications.[16] Finally, most patients with cSDH are elderly and have major

To cite: Liu Y, Madhani SI, Arturo Larco JL, *et al*. *J NeuroIntervent Surg* Epub ahead of print: [*please include* Day Month Year]. doi:10.1136/jnis-2025-023794

comorbidities that could potentially complicate general anesthesia and cranial surgery.[17 18]

Recently, two randomized controlled clinical trials (Embolization of the Middle Meningeal Artery With Onyx Liquid Embolic System for Subacute and Chronic Subdural Hematoma (EMBOLISE) and The SQUID Trial for the Embolization of the Middle Meningeal Artery for Treatment of Chronic Subdural Hematoma (STEM)) have demonstrated that adjunctive middle meningeal artery embolization (MMAe) in addition to surgery is associated with a reduction in SDH recurrence requiring reoperations, with a number needed to treat of 14.[19 20] With the increasing adoption of MMAe, the prevailing treatment paradigm for symptomatic cSDH now often involves a two step approach: surgical evacuation for rapid decompression followed by MMAe to reduce the risk of recurrence. While effective, this strategy requires two separate interventions, prolongs hospitalization, increases healthcare costs, and exposes patients (many of whom are elderly or medically fragile) to the risks associated with open surgery. A minimally invasive alternative capable of simultaneously relieving mass effect and preventing hematoma re-accumulation, ideally performed in a single session without interrupting anticoagulation or antiplatelet therapy, represents a critical and currently unmet clinical need.

We hypothesized that cSDH could be treated using a single session transvascular procedure that combines MMAe with endovascular hematoma drainage. To evaluate this concept, we conducted a multimodal preclinical feasibility study incorporating anatomical, rheological, and biomechanical analyses.

First, we generated a cSDH topographic heat map by analyzing preoperative head CT scans from patients undergoing surgical drainage of non-acute SDH. This map was used to assess the feasibility of targeting cSDH via a transvascular route. We then co-registered the heat map with DSA of the middle meningeal artery (MMA) and with segmentation of the superior sagittal sinus (SSS) from multiplanar CT images to create a composite "perforation map", to identify optimal perforation sites for subdural access.

Second, we evacuated non-acute SDH from a patient cohort using direct aspiration with small bore needles through surgically created burr holes, and then tested the ease of aspiration of collected hematoma samples using a 0.027 inch endovascular catheter routinely used in MMAe. We further conducted rheological analysis on these samples to characterize viscosity profiles and examine correlations between viscosity and radiodensity, as measured in Hounsfield units (HU), on CT.

Third, we performed structural and mechanical testing on fresh human cadaveric dura to quantify the force required for perforation using micro-scale instrumentation and to assess the geometry and behavior of the dura during controlled puncture.

MATERIALS AND METHODS

Demographic and radiological data collection

Patient demographic data, such as age at procedure, gender, history of MMAe, recurrence of SDH post-evacuation, and repeat evacuation procedure, were collected. Preoperative CT images were reviewed by a radiologist using inhouse viewing software, and SDH was classified as acute (hyperdense relative to cortex), subacute (isodense relative to cortex), chronic (hypodense relative to cortex, cSDH), acute on chronic (isodense with hematocrit level), and multiloculated if internal septations were identified.[21] The software's built-in free hand selection tool was then used to measure the average HU of the hematomas. Additionally, measurements of preoperative and postoperative maximum hematoma diameter (MHD) and midline shift diameter (MSD), using a combination of intracranial sagittal view images and radiology reports, were also collected.

Quantification of spatial distribution for SDH

To quantify the spatial distribution of SDH, we analyzed preoperative non-contrast head CTs from 69 patients with SDH to generate a three-dimensional probability heat map of hematoma occurrence across the brain surface. Five coronal planes (orbital apex, foramen rotundum, fourth ventricle, tentorial notch, and torcula) and four axial planes ("hand knob," corpus callosum, foramen of Monroe, and cerebral peduncles) were evaluated per patient (figure 1A). A polar coordinate system was applied to each plane to measure hematoma spread by angular position (azimuthal angle, θ) (figure 1B). For each scan location, the cSDH angular spread measured in all patients was collectively analyzed (figure 1C), and the probability of SDH presence as a function of θ, $P(\theta)$, was calculated. A total of nine probability functions were derived (figure 1D–F), including P_{X1}–P_{X5} for the five coronal planes, and P_{Z1}–P_{Z4} for the four axial planes.

To determine the overall probability (P_o) at any brain surface point (the asterisk in figure 1A as an example), four steps were conducted: (1) the nearest coronal (orbital apex and foramen rotundum) and axial (corpus callosum and foramen of Monroe) planes were identified; (2) the point was projected onto these four planes to derive its angular positions, θ_{X1}, θ_{X2}, θ_{Z2}, and θ_{Z3}, on the orbital apex, foramen rotundum, corpus callosum, and foramen of Monroe planes, respectively; (3) using the $P(\theta)$ functions derived above, the probability of presence in the coronal direction P_X was found by linearly interpolating $P_{X1}(\theta_{X1})$ and $P_{X2}(\theta_{X2})$, and the probability of presence in the axial direction P_Z was found by linearly interpolating $P_{Z2}(\theta_{Z2})$ and $P_{Z3}(\theta_{Z3})$; and (4) P_o was computed as the product of probabilities from both directions: $P_o = P_X P_Z$. This method synthesizes multiplanar CT data into a clinically interpretable three-dimensional heat map to visualize high risk cSDH regions. This map was used to assess the feasibility of targeting cSDH via a transvascular route.

Transvascular targeting of cSDH

We then co-registered the cSDH heat map with DSA of the MMA to generate a composite "perforation map." This allowed us to identify potential perforation sites for transvascular access to the subdural space. To estimate the maximal outer diameter of a microcatheter that could safely navigate to the MMA and to define the anticipated trajectory of the catheter on exiting the vessel into the hematoma, we performed a morphometric analysis of the MMA in 107 patients who had undergone MMAe.

Anteroposterior and lateral angiographic projections were analyzed. The MMA trunk and its posterior division were manually segmented. The perforation point was selected such that it would overlay the subdural collection and allow for a tangential trajectory from the parent vessel (mimicking the path of a microwire during perforation) to align with the convexity of the brain. The entry point into the hematoma was chosen to provide immediate access on vessel perforation, and the target point was selected to enable advancement of the catheter toward the distal boundaries of the hematoma cavity, including multiloculated regions (ie, perforation at the SDH and edge-to-edge navigation). The anticipated extravascular trajectory of the microwire in the subdural fluid was assumed to follow the segment of the MMA preceding perforation, and it was considered "appropriate" when it crossed the area with >90% probability of having SDH in the heatmap.

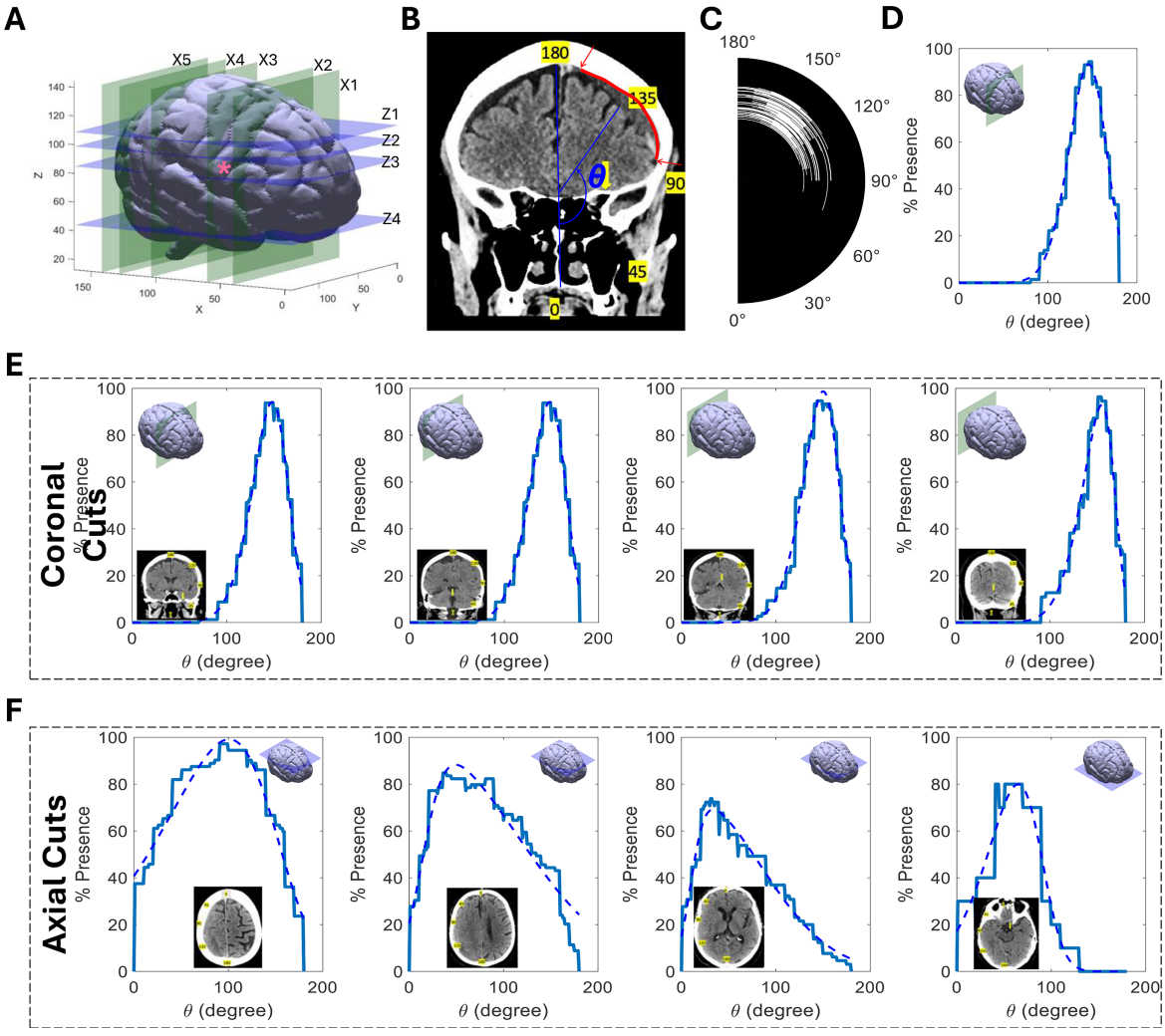

Figure 1 Generation of chronic subdural hematoma (cSDH) heat map on the brain surface. (A) For each patient, CT images at five coronal (X1–X5) and four axial (Z1–Z5) cuts were obtained and analyzed. (B) Within each CT image, taking a cut through the orbital apex as an example, a polar coordinate was established with the brain center as the origin, and location along the brain surface was mapped to azimuthal angle θ, and the minimal and maximal θ values (red arrows) were quantified. (C) Overlay of the azimuthal ranges of all of the cases for cuts through the orbital apex. (D) Probability distribution of SDH presence as a function of θ for cuts through the orbital apex; the dashed line is fitted skewed Gaussian distribution. (E) Probability distribution of SDH presence as a function of θ for the other four coronal cuts: from left to right, foramen rotundum, fourth ventricle, tentorial notch, and torcula. (F) Probability distribution of SDH presence as a function of θ for the four axial cuts: from left to right, "hand knob", corpus callosum, foramen of Monroe, and cerebral peduncles.

cSDH collection and processing

After obtaining institutional review board approval, samples of SDH from patients undergoing evacuation surgeries were collected by directly piercing the dura (after performing a burr hole or a craniotomy) with an 18 G needle (inner diameter of 0.033 inches) and aspirating with a 20 mL syringe (online supplemental video 1). The samples were stored in airtight containers and labeled with standard anonymized descriptions for reference. Ethylenediamine tetraacetic acid solution (30 mg/mL) was added to the sample to achieve a final concentration of 1.5 mg/mL to avoid clotting. For each sample, 3 mL were transferred to a separate Falcon tube for manual aspiration and viscosity testing, and the rest was stored for future use.

Manual aspiration test

The feasibility of draining a SDH via a microcatheter was studied by a manual aspiration test. Immediately after collection, SDH samples were aspirated manually using a 10 mL syringe and a microcatheter (27 Phenom, Medtronic) with a 0.027 inch inner diameter and 150 cm in length, and the time required to aspirate 3 mL of SDH was recorded (online supplemental video 2). This catheter was selected due to the relatively large lumen to enhance flow rate. Based on our clinical experience and a survey conducted with 15 neurointerventionalists, this microcatheter can be typically advanced into the intracranial MMA trunk.

Viscosity test

Viscosity of cSDH was measured within 12 hours of collection using a hybrid rheometer (DHR-1 Hybrid, TA Instruments). A single shear rate steady flow (peak hold) method was applied and the testing temperature was set at 37°C. In this method, the sample was held at shear rates of 0.1, 1, 10, 100, and 1000/s for 300 s to ensure steady state was achieved. Variable shear rates were used as the samples are non-Newtonian fluids and the viscosity is shear rate dependent. These shear rates were selected to mimic the cases from near stationary to fast aspiration by a microcatheter.

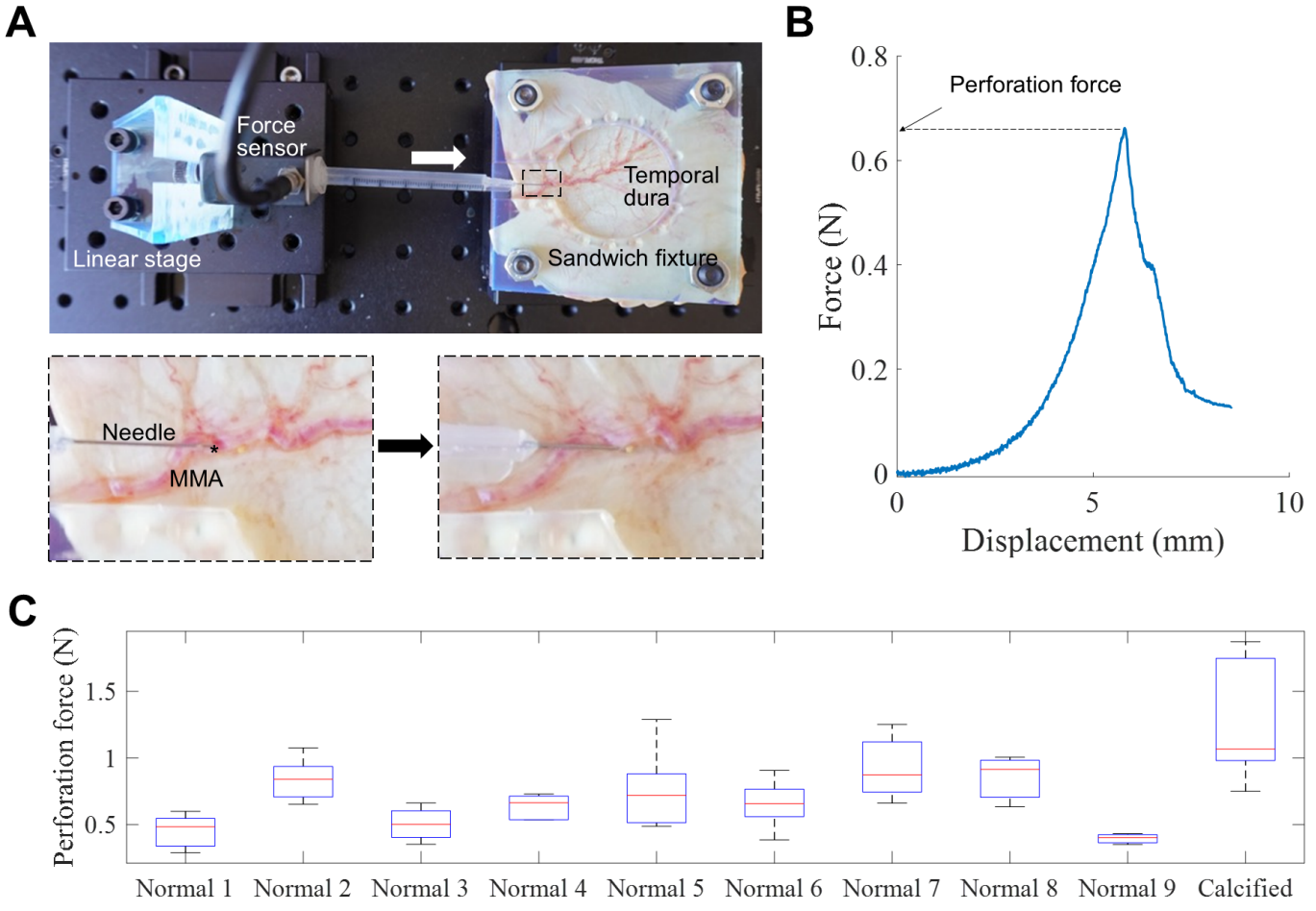

Figure 2 Needle perforation test on human dura samples. (A) Test set-up for dura and middle meningeal artery (MMA) penetration; before testing, the MMA was dissected longitudinally, and the linear stages were adjusted to aim the needle tip (asterisk) to the MMA. (B) A sample force curve with the perforation force defined as the peak force. (C) Perforation forces for nine normal and one calcified temporal dura.

Needle perforation test

To quantify the force needed to penetrate the MMA and dura to get into the subdural space, needle perforation tests were conducted in fresh cadaveric human duras. Specimens were harvested at autopsy from cadavers within 24 hours of decease and stored in 0.9% saline in a 4°C fridge before testing. The MMA was identified on the epidural surface and cut open longitudinally to expose the inner wall to mimic needle perforation from inside the MMA. The specimen was then sandwiched by a customized fixture (figure 2A), which had an inclination angle of 15° to mimic the angle of attack of a hypothetical penetrating element inside the MMA. The penetrating element in these tests was a 28 G (0.014 inch outer diameter) needle, which was fixed to a force sensor (MDB-2.5, Transducer Techniques) on a computerized linear stage assembly (PT1-Z8, Thorlabs). After aiming the needle tip at the MMA, the linear stage moved at 1 mm/s to push the needle to penetrate the MMA and dura. During this process, the force was recorded at a sampling rate of 100 Hz and the peak force was defined as the perforation force (figure 2B). In this study, nine normal dura specimens and one calcified dura specimen were tested, and for each specimen, five perforation tests were conducted.

Statistical analysis

Continuous data are expressed as mean (SD) and were compared with a Mann–Whitney U test. Correlation was evaluated using the Pearson's linear correlation coefficient. Statistical significance was indicated by $P<0.05$.

RESULTS

Patient cohort

This study involved a cohort of 38 patients undergoing surgical evacuation. Demographic and radiologic data were available for 36 patients. Mean age at the time of the procedure was 72.6 (50–93) years, 26 were men, 21 underwent MMAe (4/21 before evacuation surgery, 17/21 after evacuation surgery), 6 patients had recurrence of SDH post-evacuation surgery, and 2 patients underwent repeat evacuation surgery. Forty-four SDH samples were collected; 34 samples by direct aspiration with the needle through the dura (77%) and 10 samples after widely opening the dura, membranes, and trabeculations (23%). Viscosity and manual aspiration testing were available for 41 and 16 samples, respectively.

Radiologic data

The SDH samples included 4 acute SDH, 5 subacute SDH, 17 cSDH, and 18 acute on chronic SDH (table 1), and 32% were multiloculated (n=14). For this cohort, average HU of hematoma, baseline MHD, and baseline MSD were 36.1 (SD 11.6), 16.9 (SD 6.4) mm, and 5.9 (SD 4.7) mm, respectively. After surgical evacuation, decreases in MHD and MSD were 7.6 (SD 6.5) mm and 2.5 (SD 2.5) mm, respectively. Intergroup

Table 1 Analysis of the radiologic characteristics by subdural hematoma (SDH) type

SDH type	No of patients	HU	Baseline MHD (mm)	Baseline MSD (mm)	Decrease in MHD (mm)	Decrease in MHD (mm)
Acute	4	50.9 (12.5)	16.7 (7.1)	6.8 (5.4)	6.5 (2.3)	2.0 (1.4)
Subacute	5	41.0 (7.2)	10.9 (6.1)	NA*	5.0 (5.0)	NA
Chronic	17	33.4 (13.3)	16.2 (6.9)	5.7 (5.0)	6.5 (8.2)	2.0 (2.0)
Acute on chronic	18	33.9 (7.7)	18.8 (5.4)	7.2 (4.0)	9.4 (5.4)	3.9 (2.6)

*No baseline midline shift was noted in any patient.
HU, Hounsfield unit; MHD, maximum hematoma diameter; MSD, midline shift diameter.

differences were not statistically significant except: (1) average HU was larger for acute SDH than for acute on chronic SDH (P=0.01); and (2) MHD was larger for acute on chronic SDH than for subacute SDH (P=0.04).

Topographic heat map of cSDH

The probability of cSDH presence was calculated, represented using a heat map continuum (red=100%, blue=0% probability), and presented on a template brain mesh model (figure 3A). The highest probability zones (>80%) localized to parietal and frontal convexities. Low probability (~10%) zones localized to the temporal lobes and occipital regions. Probabilities decayed sharply to near zero values in midline region, parasagittal zones and at the skull base. Given this near zero probability of SDH presence in the midline and parasagittal zones, further analysis of transvascular access from the SSS was not conducted.

MMA morphology and perforation trajectory

The main morphological characteristics of the MMA found in this study were: (1) the MMA angle at the foramen spinosum was 100° (SD 14°); (2) the MMA groove along the concave middle cranial fossa followed an angle of 160° (SD 5.8°); (3) the intracranial segment of the MMA trunk had a mean diameter of 1.48 mm (SD 0.19 mm); (4) the proximal anterior division of the MMA had a mean diameter of 1.01 mm (SD 0.12 mm); and (5) the proximal posterior division of the MMA had a mean diameter of 1.23 mm (SD 0.23 mm). Of the 107 cases, the microwire was estimated to be able to perforate over the SDH in 105 cases by selecting an appropriate perforating point (figure 3B), with a highly probable (>70%) appropriate edge-to-edge trajectory.

SDH viscosity

SDH viscosity demonstrated a shear rate dependent behavior, decreasing with the shear rate, with a plateau at high shear rates (figure 4A). For each shear rate, intergroup differences were not statistically significant except for the viscosity of acute on chronic SDH which was higher than for cSDH (P=0.02). To describe the non-Newtonian behavior, the Carreau model was applied, which is defined as follows:

$$\eta = \eta_\infty + (\eta_0 - \eta_\infty)\left(1 + \lambda^2\gamma^2\right)^{\frac{n-1}{2}}$$

where η is dynamic viscosity, η_∞ is infinite shear viscosity, η_0 is zero shear viscosity, λ is relaxation time, γ is shear rate, and n is the power law index. Such a model has been used to model the non-Newtonian behavior of human blood and demonstrated good fidelity.[22] For this cohort of SDH samples, the fitted model parameters were: η_∞ = 2.78 mPa×s, η_0=172 mPa×s, λ=2.43 s, and n=0.124. The SDH was more viscous than blood at low shear rates and less viscous at high shear rates (figure 4B).

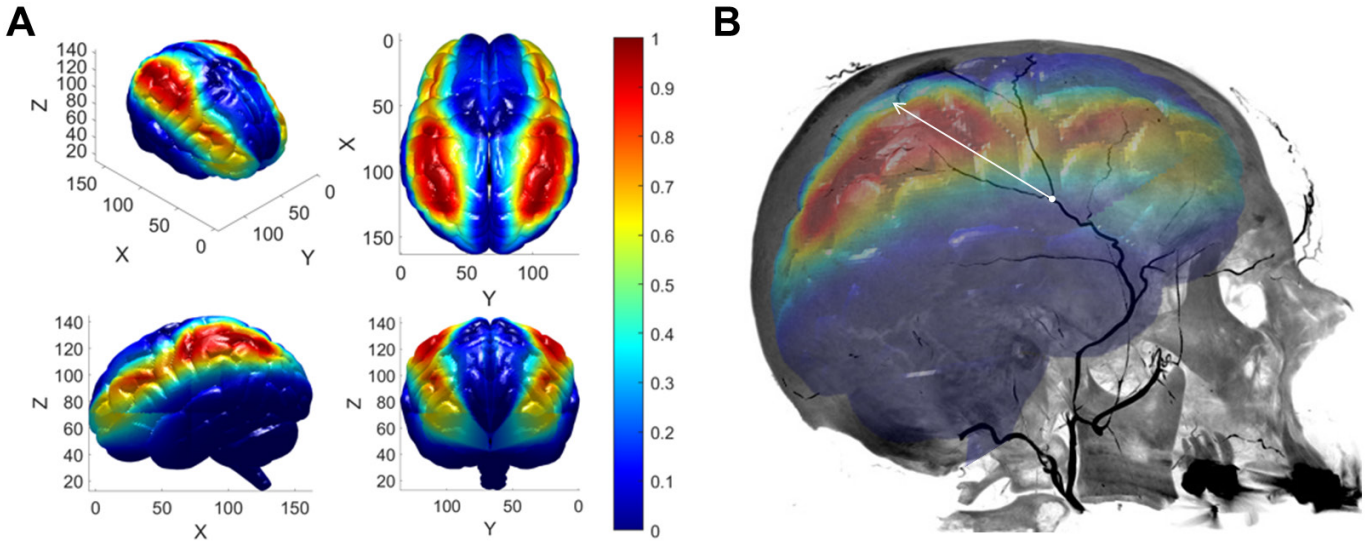

Figure 3 Anatomical analysis of chronic subdural hematoma (cSDH) distribution, middle meningeal artery (MMA) perforation site, and microwire trajectory after perforation. (A) Oblique and projection views of the three-dimensional heat map of cSDH distribution on the brain surface. (B) SDH heatmap was overlayed with the patient's MMA angiogram, and the edge-to-edge trajectory of the microwire (white arrow) was then drawn between the entry point at the perforation site and the opposite SDH edge.

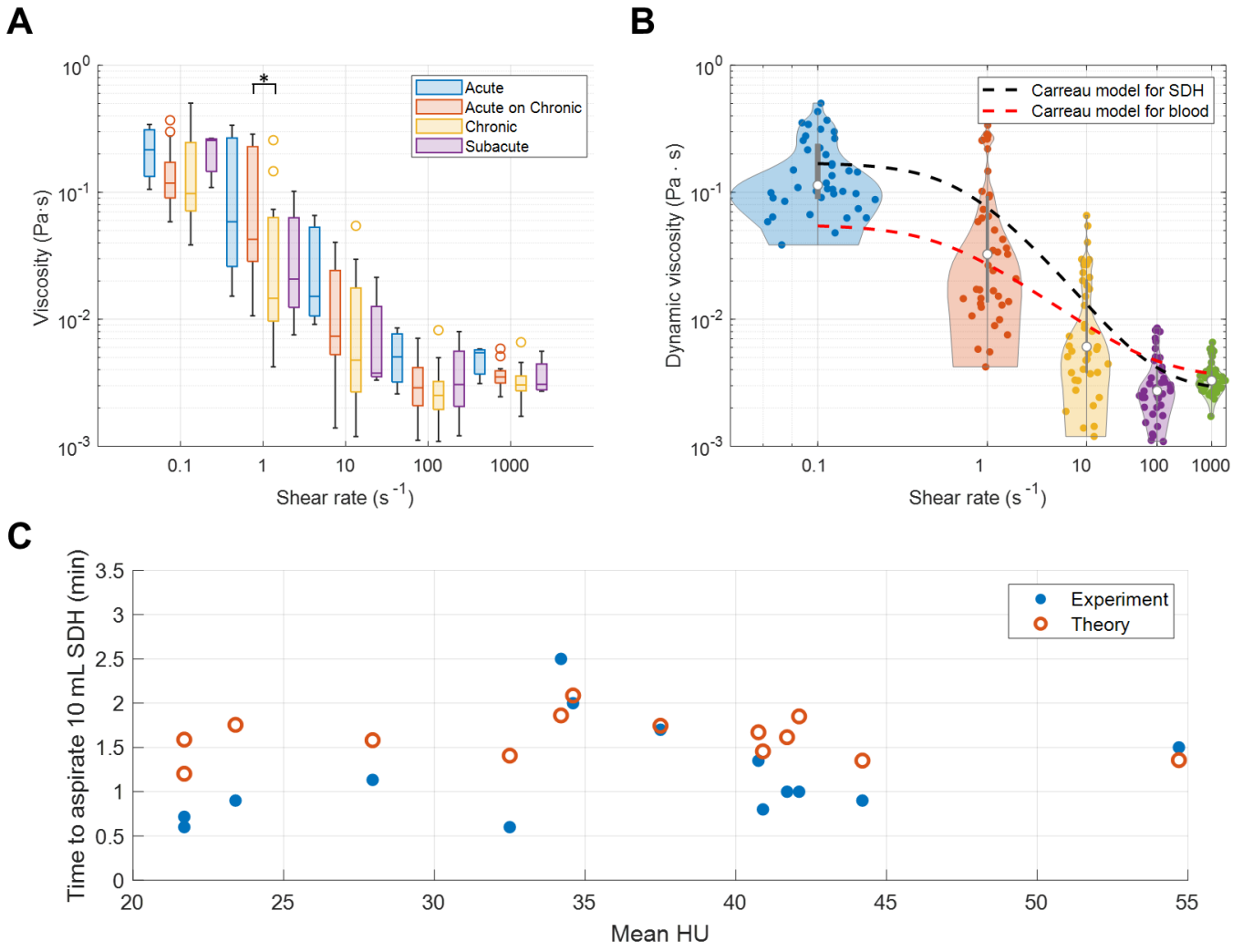

Figure 4 Rheological analysis of subdural hematoma (SDH) samples. (A) Viscosity versus shear rate for samples grouped by SDH type (*P<0.05). (B) Viscosity data fitted by the Carreau model and compared with human blood. (C) Empirical and theoretical aspiration time and their relations to mean Hounsfield unit (HU) for SDH samples.

SDH aspiration time

From the aspiration experiment, the time needed to aspirate 10 mL ranged from 0.6 to 2.5 min (1.21±0.54 min) (figure 4C). The aspiration time showed an increasing trend with the HU value, but the correlation was not statistically significant (r=0.24, P=0.38).

Aspiration time was also estimated using the measured viscosity. First, to determine if the aspiration flow of SDH within the microcatheter was laminar or turbulent, the Reynolds number was calculated for all of the tests and was found to be <2300, the threshold of the flow transitioning to turbulence. Therefore, the Hagen–Poiseuille equation was used to calculate the aspiration flow rate for cSDH:

$$Q = \frac{\pi D^4 P}{128 \eta L}$$

where Q is aspiration flow rate, D is inner diameter of the microcatheter, P is magnitude of vacuum pressure applied for aspiration, and L is length of the microcatheter. To select the appropriate value of η for calculation, the shear rate of the aspiration flow was estimated using the empirical flow rates, and all were >1000/s. Therefore, the viscosity at the shear rate of 1000/s was selected to calculate the theoretical flow rates. The theoretical aspiration time showed relatively good agreement with the experimentally measured time (figure 4C). The averaged relative error between the theoretical and empirical results was 68%. Such an error was mainly due to the assumption that the viscosity of the SDH flowing inside the microcatheter was the same as that flowing with 1000/s shear rate, while the actual shear rate can only be roughly estimated and varied among different cases.

Perforation force for MMA and Dura

For the normal temporal dura, needle penetration force ranged from 0.29 to 1.29 N (0.68±0.24) (figure 2C). In comparison, the needle penetration force for the calcified dura ranged from 0.75 to 1.87 N (1.29±0.48). The needle perforation force for the calcified dura was significantly (P=0.05) larger than that for normal ones.

DISCUSSION

Our study provides foundational preclinical evidence supporting the feasibility of a fully endovascular approach for the treatment of non-acute SDH. Recently, the management of symptomatic cSDH has relied on a two step paradigm involving surgical evacuation for immediate decompression followed by MMAe to reduce recurrence risk. While clinically effective, this sequential approach is resource intensive, prolongs hospitalization, and

poses increased risks for elderly and anticoagulated patients. In contrast, our data demonstrated that a single session transvascular procedure (integrating both embolization and catheter based hematoma drainage) is plausible. Using multimodal analysis, we identified consistent SDH topography aligned with accessible MMA perforation trajectories, confirmed that hematoma viscosity is compatible with microcatheter aspiration, and quantified the mechanical forces required to safely perforate the dura. Together, these findings establish critical design parameters and procedural considerations for future translational development of this minimally invasive strategy.

First, we demonstrated that cSDH can be drained at clinically acceptable flow rates by small lumen catheters. In our cohort, drainage with a syringe and needle enabled successful sample collection in all unselected, consecutive cases. The capacity to drain different non-acute SDH is consistent with extensive clinical experience reported in China, where the YL-1 hollow needle aspiration drainage system has been widely used for the treatment of non-acute SDH over the past two decades.[23] This system uses a 3 mm diameter, 2 cm long needle, implanted into the skull using a power drill to enable continuous drainage over an average duration of 2.5 days and is often augmented with urokinase instillation. In a large retrospective series of 697 patients, this technique achieved a success rate exceeding 97%, with an acceptable complication profile, including a 5% incidence of acute subdural or epidural hematomas related to the implantation procedure.[24] These findings are further corroborated by Yamamoto *et al*, who reported favorable outcomes using percutaneous 23 G butterfly needles (0.025 inch outer diameter, 0.013 inch inner diameter, 19 mm length) to evacuate recurrent SDH through pre-existing burr holes, achieving drainage rates of approximately 5 mL/min and immediate symptom relief.[25] Together, these data support the premise that non-acute SDH can be effectively accessed and drained via small caliber instruments, laying the groundwork for minimally invasive, catheter based approaches.

Building on these foundational observations, we empirically tested catheter based drainage using a 0.027 inch inner diameter microcatheter (150 cm in length), which successfully aspirated surgically collected SDH samples at an average rate of 8.3 mL/min. This catheter was chosen because it represents the largest profile that can be reliably navigated into the intracranial MMA and its primary divisions.

To further understand how catheter design influences drainage performance, we performed rheological analysis of the SDH samples and modeled flow dynamics using Poiseuille's law. Theoretical aspiration times calculated from viscosity data were approximately 68% slower than the observed empirical rates, likely due to the challenges in accurately estimating shear rate within the microcatheter lumen and the shear thinning nature of the SDH fluid. These findings suggest that optimizing catheter geometry, particularly through tapering, could substantially improve flow rates. Specifically, a catheter design with a distal inner diameter of 0.027 inches and a proximal diameter of 0.050 inches could theoretically drain 10 mL of SDH in approximately 5 s. These results underscore the importance of tailored catheter engineering to maximize efficiency and safety in future transvascular SDH drainage systems.

Anatomic feasibility was further supported by the cSDH topography heat map and probabilistic trajectory analysis of MMA perforation points. Based on our morphometric analysis, and assuming a Gaussian distribution of the artery diameter and neglecting the navigation difficulty posed by tortuous anatomy, a microcatheter with a distal outer diameter of 1 mm (0.039 inches/3 F) should be able to navigate in the proximal anterior or posterior division in >53% of patients, while a microcatheter with a distal outer diameter of 0.75 mm (or 0.030 inches/2.25 F) should be able to navigate in the proximal anterior or posterior division of the MMA in >98% of patients. Perforations in those arterial segments would have resulted in highly probable (>70%) appropriate edge-to-edge trajectory. The trajectory: (1) was assumed to be an extension of the trajectory of the MMA segment immediately proximal to the perforation point; (2) starts at the transvascular entry point (perforation point) at the anterolateral SDH margin; (3) extends in the subdural space crossing the area with >90% probability of having SDH; and (4) reaches a final target point at the posterior and medial SDH margin. The capacity to advance inside the SDH from one edge to the other, and into different pockets across septations, would likely increase the likelihood of successful drainage, especially in multiloculated SDH. In our tests, the collection of about 25% of the samples required wide incision of the dura and membranes and fenestration of septations within the SDH to collect the preset 20 mL.

In this study, we also considered the feasibility of draining the SDH via a transvenous route through the SSS. Transvenous access to the intradural space has precedent, most notably in the implantation of the eShunt (CereVasc) for the treatment of communicating hydrocephalus, as demonstrated by Lylyk and colleagues.[26] Venous access offers advantages, including larger vessel diameters and lower intraluminal pressures compared with arteries. However, our cSDH heat map analysis revealed that the probability of non-acute hematomas directly abutting the SSS wall was very low. Thus any transvenous approach would require perforation of the sinus wall followed by navigation over the brain surface before reaching the hematoma, raising safety concerns. Additionally, the lateral walls of the SSS are traversed by numerous bridging veins, which are poorly visualized on conventional angiography and may be inadvertently injured during perforation, increasing the risk of iatrogenic hemorrhage. Venous wall perforation would also necessitate a closure strategy to mitigate the risk of persistent bleeding, and the use of such a device could jeopardize sinus patency, with potentially serious clinical consequences. Furthermore, transvenous drainage would not eliminate the need for arterial access and MMAe, thereby duplicating procedural steps, equipment, and associated risks.

In contrast, as demonstrated here, the MMA can provide a consistent anatomical pathway to perforate over the hematoma cavity in most cases. This "landing zone" in the subdural fluid would theoretically increase the safety profile of a transvascular access, as the brain is displaced ("protected") by the SDH. This unique anatomy is highly consistent among different patients, as the MMA always follows the inner surface of the skull, and the SDH is always between the dura and the brain. Furthermore, the MMA is a vessel known to tolerate occlusion well, particularly in this patient population, where embolization is already therapeutic and known to decrease the likelihood of recurrent SDH. Collectively, these anatomical and procedural considerations strongly favor a transarterial approach, where embolization and drainage can be seamlessly integrated into a single, minimally invasive intervention.

In this study, we performed a mechanical analysis of human dura and quantified the forces required for penetration. Although this analysis was performed on fresh cadaveric tissue, we contend that the findings are highly applicable to in vivo conditions. The dura mater consists of dense connective tissue, with mechanical strength primarily derived from its compact collagen layers, thereby minimizing the influence of absent blood flow and vascular tone. The dura is a highly resistant

tissue that demands both sharp instrumentation and substantial axial force for successful perforation. This introduces a key technical challenge: while sharper tips can lower the required penetration force, they also increase the risk of catheter skiving along vessel curvatures, potentially resulting in unintended brain injury. Conversely, higher perforation forces necessitate devices with increased column strength and pushability, typically achieved through stiffer materials, but such constructs are often incompatible with the tortuous geometry of the intracranial vasculature. This technical challenge is significantly amplified in cases of dural calcification, which we found to require substantially higher perforation forces. This represents a critical worst case scenario that should inform the design of perforation mechanisms. Additionally, advanced intraoperative imaging modalities, such as flat panel CT, warrant exploration to help in the selection of optimal perforation points. These opposing demands underscore the need for a highly specialized delivery system; one that is both sufficiently small and flexible to navigate through the intracranial circulation, but capable of precise and controlled dural perforation. These engineering requirements provide important design parameters for the development of future transvascular devices aimed at accessing the subdural space safely and effectively.

In summary, this study has established the foundational principles supporting the feasibility of transvascular drainage for chronic subdural hematoma. Clinical translation of this approach will require the development of dedicated endovascular systems that combine tapered geometries for efficient aspiration, hybrid flexibility–stiffness profiles for reliable navigation through the MMA, and engineered tip designs capable of controlled and reproducible dural perforation. While further investigation is necessary to assess procedural safety and optimize device design, our anatomical, rheological, and mechanical analyses collectively support endovascular SDH evacuation as a viable and minimally invasive alternative to conventional surgery.

This study had several limitations. First, the mechanical analysis of dural perforation was conducted using fresh cadaveric tissue, which may not fully replicate the biomechanical behavior of living dura. Second, although we observed significantly higher perforation forces in calcified dura, reliably identifying such focal calcifications preoperatively remains a clinical challenge. Third, the feasibility of transvascular access requires evaluation in vivo to assess biological responses. These factors represent important avenues for future investigation as this approach advances toward clinical translation.

CONCLUSIONS

This study provides objective evidence supporting the feasibility of a transvascular approach for the drainage of non-acute subdural hematomas. Our findings identified key technical enablers, including anatomical concordance between cSDH distribution and accessible MMA perforation trajectories, rheological properties of hematoma fluid amenable to microcatheter aspiration, and dural perforation forces within practical, achievable ranges. Collectively, these results establish a foundational framework for advancing cSDH management toward a minimally invasive, single session endovascular strategy.

X Sarosh Irfan Madhani @MadhaniSarosh, Jorge Luis Arturo Larco @JLarco8 and Yigit Can Senol @yigitcs

Contributors YL and LS conceptualized and designed this study. YL led the study conduction and manuscript drafting. SIM, JLAL, AHS, YCS, and PNL contributed to data collection and analysis. LS supervised the overall project and provided major input in manuscript development. YL and LS are the guarantors of this study.

Funding This work was supported by the National Natural Science Foundation of China (52405282), Science and Technology Commission of Shanghai Municipality (23YF1420900), NIH Blueprint MedTech Incubator (CA-0243420-20240601), and Mayo Clinic Translational Product Development Fund (TPDF-FP00114027).

Competing interests YL: inventor of awarded and pending patent applications related to the technology of subdural hematoma (SDH) drainage and licensed to Endovascular Horizons. LES: inventor of awarded and pending patent applications related to the technology of SDH drainage and licensed to Endovascular Horizons; founder of Endovascular Horizons; and stock or stock options in Endovascular Horizons.

Patient consent for publication Not applicable.

Ethics approval The study was approved by the institutional review board at Mayo Clinic (Rochester, Minnesota): IRB 20-002480 and IRB 20-001299.

Provenance and peer review Not commissioned; externally peer reviewed.

Data availability statement Data are available upon reasonable request.

ORCID iDs
Yang Liu http://orcid.org/0000-0002-9132-0258
Sarosh Irfan Madhani http://orcid.org/0000-0003-4855-8487
Adnan Hussain Shahid http://orcid.org/0000-0003-2703-3497
Yigit Can Senol http://orcid.org/0000-0002-6669-6616

REFERENCES

1 Ducruet AF, Grobelny BT, Zacharia BE, *et al*. The surgical management of chronic subdural hematoma. *Neurosurg Rev* 2012;35:155–69.
2 Balser D, Farooq S, Mehmood T, *et al*. Actual and projected incidence rates for chronic subdural hematomas in United States Veterans Administration and civilian populations. *J Neurosurg* 2015;123:1209–15.
3 Abe Y, Maruyama K, Yokoya S, *et al*. Outcomes of chronic subdural hematoma with preexisting comorbidities causing disturbed consciousness. *J Neurosurg* 2017;126:1042–6.
4 Miranda LB, Braxton E, Hobbs J, *et al*. Chronic subdural hematoma in the elderly: not a benign disease. *J Neurosurg* 2011;114:72–6.
5 Masaaki U, Hiroyuki T, Satoshi H. Is this Disease Benign? Risk Factors in Elderly Patients. *Neurol Med Chir (Tokyo)* 2017;57:402–9.
6 Dumont TM, Rughani AI, Goeckes T, *et al*. Chronic subdural hematoma: a sentinel health event. *World Neurosurg* 2013;80:889–92.
7 Mehta V, Harward SC, Sankey EW, *et al*. Evidence based diagnosis and management of chronic subdural hematoma: A review of the literature. *J Clin Neurosci* 2018;50:7–15.
8 Weigel R, Schmiedek P, Krauss JK. Outcome of contemporary surgery for chronic subdural haematoma: evidence based review. *J Neurol Neurosurg Psychiatry* 2003;74:937–43.
9 Almenawer SA, Farrokhyar F, Hong C, *et al*. Chronic subdural hematoma management: a systematic review and meta-analysis of 34,829 patients. *Ann Surg* 2014;259:449–57.
10 Ivamoto HS, Lemos HPJ, Atallah AN. Surgical Treatments for Chronic Subdural Hematomas: A Comprehensive Systematic Review. *World Neurosurg* 2016;86:399–418.
11 Liu W, Bakker NA, Groen RJM. Chronic subdural hematoma: a systematic review and meta-analysis of surgical procedures. *J Neurosurg* 2014;121:665–73.
12 Xu C-S, Lu M, Liu L-Y, *et al*. Chronic subdural hematoma management: clarifying the definitions of outcome measures to better understand treatment efficacy - a systematic review and meta-analysis. *Eur Rev Med Pharmacol Sci* 2017;21:809–18.
13 Gernsback J, Kolcun JPG, Jagid J. To Drain or Two Drains: Recurrences in Chronic Subdural Hematomas. *World Neurosurg* 2016;95:447–50.
14 Tempaku A, Yamauchi S, Ikeda H, *et al*. Usefulness of interventional embolization of the middle meningeal artery for recurrent chronic subdural hematoma: Five cases and a review of the literature. *Interv Neuroradiol* 2015;21:366–71.
15 Ding H, Liu S, Quan X, *et al*. Subperiosteal versus Subdural Drain After Burr Hole Drainage for Chronic Subdural Hematomas: A Systematic Review and Meta-Analysis. *World Neurosurg* 2020;136:90–100.
16 Ban SP, Hwang G, Byoun HS, *et al*. Middle Meningeal Artery Embolization for Chronic Subdural Hematoma. *Radiology* 2018;286:992–9.
17 Uno M, Toi H, Hirai S. Chronic Subdural Hematoma in Elderly Patients: Is This Disease Benign? *Neurol Med Chir (Tokyo)* 2017;57:402–9.

18 Toi H, Kinoshita K, Hirai S, *et al*. Present epidemiology of chronic subdural hematoma in Japan: analysis of 63,358 cases recorded in a national administrative database. *J Neurosurg* 2018;128:222–8.
19 Davies JM, Knopman J, Mokin M, *et al*. Adjunctive Middle Meningeal Artery Embolization for Subdural Hematoma. *N Engl J Med* 2024;391:1890–900.
20 Fiorella D, Monteith SJ, Hanel R, *et al*. Embolization of the Middle Meningeal Artery for Chronic Subdural Hematoma. *N Engl J Med* 2025;392:855–64.
21 Brant WE, Helms CA. *Fundamentals of diagnostic radiology*. 4th edn. Lippincott Williams & Wilkins, 2012.
22 Moradicheghamahi J, Sadeghiseraji J, Jahangiri M. Numerical solution of the Pulsatile, non-Newtonian and turbulent blood flow in a patient specific elastic carotid artery. *Int J Mech Sci* 2019;150:393–403.
23 Zhang HZ, Wu W, She L, *et al*. Risk prognosis factors of chronic subdural hematoma evacuated by the novel YL-1 hollow needle aspiration drainage system. *J Neurosurg Sci* 2014;58:29–36.
24 Chen L, Dong L, She L, *et al*. Treatment of chronic subdural hematoma by novel YL-1 hollow needle aspiration drainage system (697 cases report). *Neurol Sci* 2017;38:109–13.
25 Yamamoto S, Nagashima Y, Maki H, *et al*. Butterfly needle tap and suction (BTS) technique: a treatment for recurrent chronic subdural hematoma after burr hole craniostomy. *Acta Neurochir (Wien)* 2023;165:841–8.
26 Lylyk P, Lylyk I, Bleise C, *et al*. First-in-human endovascular treatment of hydrocephalus with a miniature biomimetic transdural shunt. *J Neurointerv Surg* 2022;14:495–9.